Cell

Poly(ADP-Ribose) Polymerase 1 Participates in the Phase Entrainment of Circadian Clocks to Feeding

Gad Asher,[1,*] Hans Reinke,[2,5] Matthias Altmeyer,[3,4,5] Maria Gutierrez-Arcelus,[1] Michael O. Hottiger,[3] and Ueli Schibler[1,*]

[1]Department of Molecular Biology, University of Geneva, 1211 Geneva 4, Switzerland
[2]Institute for Clinical Chemistry and Laboratory Diagnostics, Heinrich-Heine-University, Medical School, Institute for Molecular Preventive Medicine at the Heinrich-Heine-University (IUF), Düsseldorf 40225, Germany
[3]Institute of Veterinary Biochemistry and Molecular Biology
[4]Life Science Zurich Graduate School, Molecular Life Science Program
University of Zurich, Zurich 8057, Switzerland
[5]These authors contributed equally to this work
*Correspondence: gad.asher@unige.ch (G.A.), ueli.schibler@unige.ch (U.S.)
DOI 10.1016/j.cell.2010.08.016

SUMMARY

Circadian clocks in peripheral organs are tightly coupled to cellular metabolism and are readily entrained by feeding-fasting cycles. However, the molecular mechanisms involved are largely unknown. Here we show that in liver the activity of PARP-1, an NAD^+-dependent ADP-ribosyltransferase, oscillates in a daily manner and is regulated by feeding. We provide biochemical evidence that PARP-1 binds and poly(ADP-ribosyl)ates CLOCK at the beginning of the light phase. The loss of PARP-1 enhances the binding of CLOCK-BMAL1 to DNA and leads to a phase-shift of the interaction of CLOCK-BMAL1 with PER and CRY repressor proteins. As a consequence, CLOCK-BMAL1-dependent gene expression is altered in PARP-1-deficient mice, in particular in response to changes in feeding times. Our results show that *Parp-1* knockout mice exhibit impaired food entrainment of peripheral circadian clocks and support a role for PARP-1 in connecting feeding with the mammalian timing system.

INTRODUCTION

Physiology and behavior of light-sensitive organisms are subject to circadian oscillations that are driven by endogenous biological clocks. In mammals, a central pacemaker in the suprachiasmatic nucleus (SCN) of the brain synchronizes slave oscillators in peripheral organs. Circadian clocks can measure time only approximately and must therefore be readjusted every day by external time cues (*Zeitgebers*) in order to stay in resonance with geophysical time (Reppert and Weaver, 2002). Although light is the predominant *Zeitgeber* for the central clock in the SCN, feeding rhythms are strong *Zeitgebers* for peripheral clocks in many tissues (Damiola et al., 2000; Stokkan et al., 2001). It is therefore likely that the SCN synchronizes peripheral oscillators at least in part by imposing rest-activity rhythms and thus feeding-fasting cycles.

Both master and subsidiary oscillators are believed to utilize a similar clock gene circuitry for rhythm generation (Yagita et al., 2001). This molecular clockwork seems to rely on the interplay between transcriptional activators and repressors that generate a negative feedback loop of core clock gene expression (Hardin et al., 1990). CLOCK-BMAL1 heterodimers bind to E box motifs present in the *Per* and *Cry* genes and stimulate their transcription. Once PER and CRY proteins reach a critical concentration and/or activity, they form a complex with CLOCK-BMAL1 and repress the transcription of their own gene loci. In addition, interconnecting feedback loops involving orphan nuclear receptors of the REV-ERB and ROR families coregulate the expression of core clock genes (Preitner et al., 2002; Sato et al., 2004).

Several lines of evidence suggest a strong interplay between metabolism and the circadian clock. The dominance of feeding cycles as *Zeitgebers* (ZTs) for peripheral clocks implies that circadian oscillations play an important role in nutrient processing and energy homeostasis (Damiola et al., 2000; Stokkan et al., 2001). Indeed, transcriptome profiling studies revealed that many genes involved in metabolic control are rhythmically expressed (Green et al., 2008). Whereas several aspects of circadian metabolism have been elucidated, little is known regarding the molecular mechanisms that adjust body clocks to the cellular metabolic state.

Accumulating evidence suggests that cellular NAD^+/NADH levels, which are generally considered as readouts of cellular metabolic states, regulate the function of the circadian oscillator. At least in vitro the DNA-binding activities of CLOCK-BMAL1 are strongly affected by $NAD(P)^+$/NAD(P)H levels (Rutter et al., 2001). Furthermore, SIRT1, an NAD^+-dependent deacetylase, binds to CLOCK-BMAL1 and regulates circadian gene expression through the covalent modification of clock transcription factors and chromatin-associated proteins (Asher et al., 2008; Nakahata et al., 2008). Subsequent studies corroborated the connection between NAD^+/NADH levels and the circadian clock by showing that nicotinamide phosphoribosyltransferase (NAMPT), the
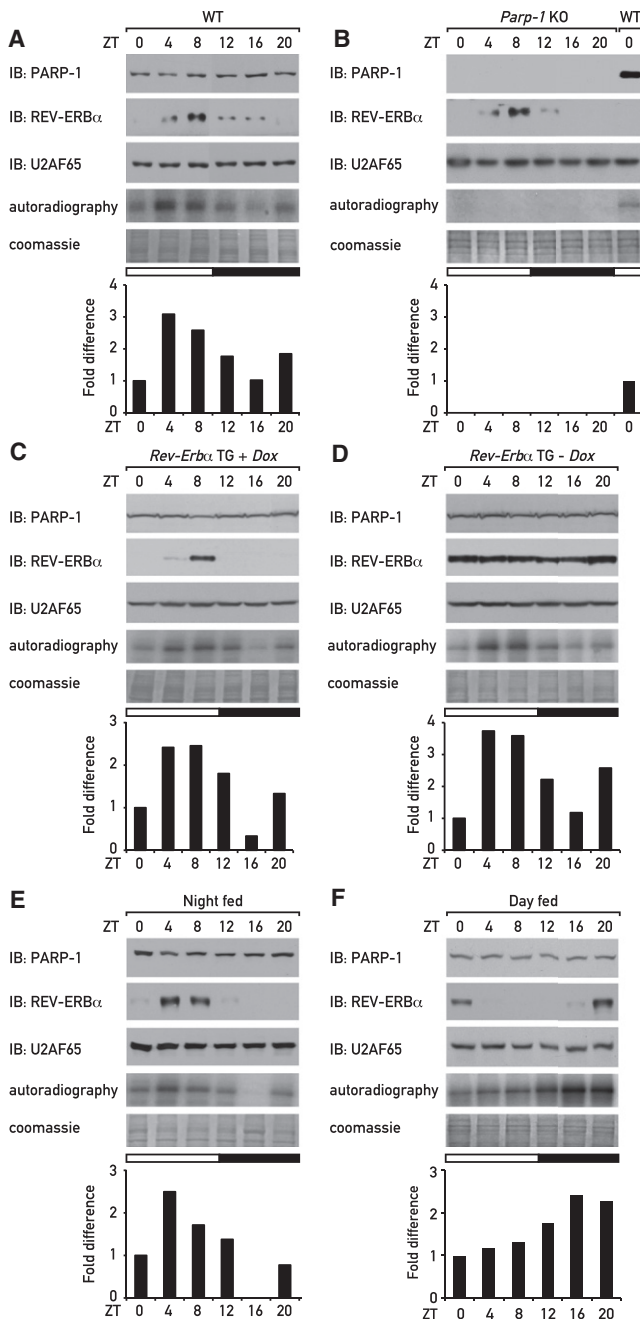
Figure 1. Analysis of Circadian PARP-1 Expression and Auto-ADP-Ribosylation Levels

Mice were sacrificed at 4 hr intervals around the clock and liver nuclear protein extracts were prepared. Protein levels of PARP-1, REV-ERBα, and U2AF65 were analyzed by immunoblotting (IB). Auto-ADP-ribosylation levels of endogenous PARP-1 (autoradiography) were analyzed with nuclear extracts obtained from (A) wild-type (WT) mice fed ad libitum, (B) *Parp-1* knockout (*Parp-1* KO) mice fed ad libitum, (C) mice expressing a *Rev-Erbα* transgene in the liver under negative control of tetracycline (*Rev-Erbα* TG) fed ad libitum with doxycycline (+Dox) (liver clock operative), (D) *Rev-Erbα* TG mice fed ad libitum without doxycycline (−Dox) (liver clock arrested), (E) wild-type mice fed exclusively during the dark phase (Night fed), (F) wild-type mice fed exclusively during the light phase (Day fed). ZT is the *Zeitgeber* time; white and dark bars indicate light

rate-limiting enzyme of the NAD$^+$ salvage pathway, is expressed in a circadian manner and generates daily oscillations of NAD$^+$ levels (Nakahata et al., 2009; Ramsey et al., 2009).

The mounting evidence supporting the involvement of NAD$^+$-dependent enzymes in the clockwork circuitry encouraged us to test whether PARP-1 (poly(ADP-ribose) polymerase 1), an NAD$^+$-dependent ADP-ribosyltransferase (Altmeyer and Hottiger, 2009; Hassa and Hottiger, 2008; Schreiber et al., 2006), also executes circadian functions. PARP-1 modulates the activities of several transcriptional regulatory proteins either by direct protein-protein interaction or by NAD$^+$-dependent poly(ADP-ribosyl)ation (Hassa et al., 2006; Petesch and Lis, 2008). Interestingly, ADP-ribosylation has already been implicated in circadian gene expression in plants (Dodd et al., 2007; Panda et al., 2002).
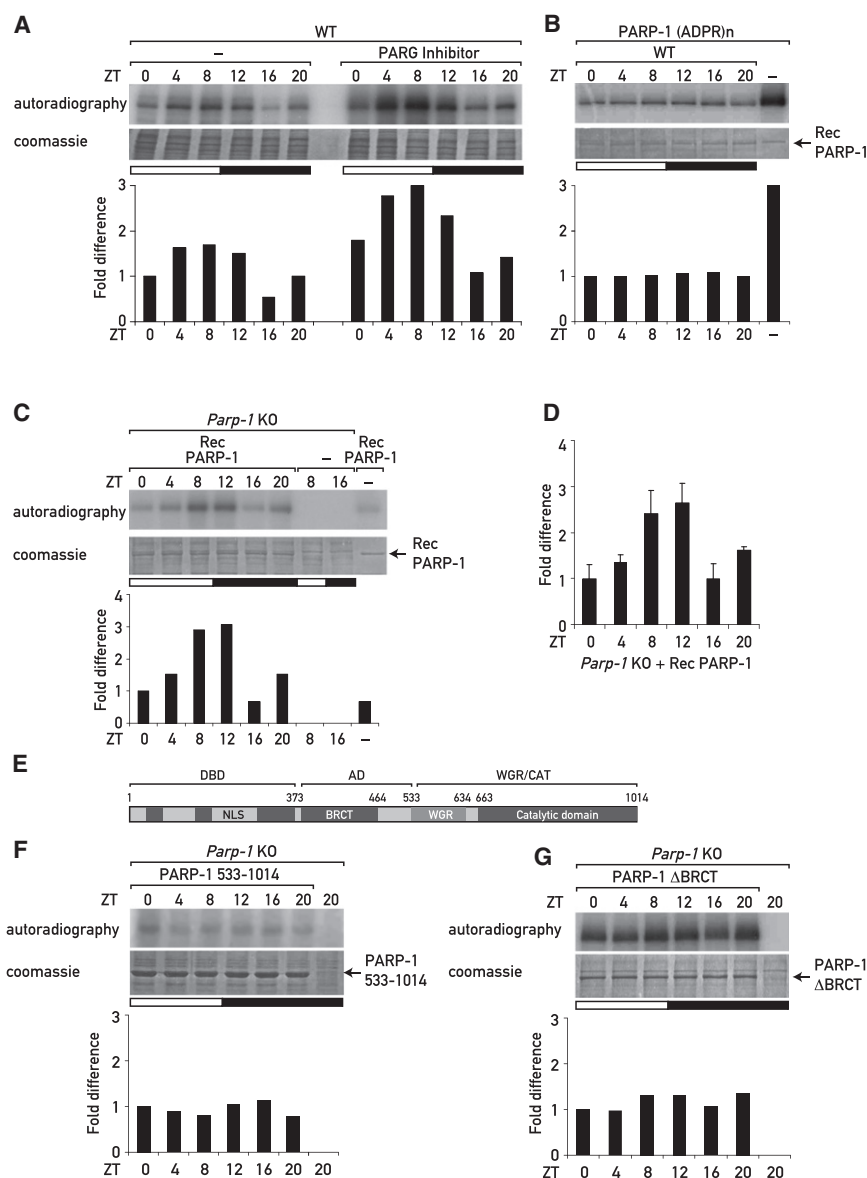
Here we show that in mouse liver PARP-1 poly(ADP-ribosyl)ation activity is circadian and regulated by feeding. PARP-1 binds to CLOCK-BMAL1 heterodimers and poly(ADP-ribosyl)ates CLOCK in a daily manner. Poly(ADP-ribosyl)ation of CLOCK modulates the DNA-binding activity of CLOCK-BMAL1 and its interaction with components of the negative limb, the PER and CRY proteins, which in turn alters circadian gene expression. Remarkably, the entrainment of liver clocks to inverted feeding is significantly delayed in the absence of PARP-1.

RESULTS

PARP-1 Activity in Mouse Liver Is Rhythmic and Regulated by Feeding

To address a potential role for PARP-1 in circadian clock control, we first analyzed the pattern of expression and auto-ADP-ribosylation of PARP-1 in mouse liver. Mice were sacrificed at 4 hr intervals around the clock, and liver nuclear extracts were prepared. Whereas nearly constant levels of nuclear PARP-1 protein were observed around the day (Figure 1A), NAD$^+$-dependent auto-ADP-ribosylation of PARP-1 measured in vitro was highly circadian with a maximum around ZT4 (Figure 1A and Figure S1A available online). The identity and requirement for PARP-1 in the ADP-ribosylation reactions were confirmed both by performing the assay with nuclear extracts obtained from *Parp-1* knockout mice (Figure 1B) and by addition of different PARP inhibitors (Figures S1B and S1C). To address whether rhythmic auto-ADP-ribosylation of PARP-1 also occurs in vivo, immunoprecipitation experiments were performed with poly(ADP-ribose) antibodies and then analyzed with PARP-1 antibody. Similar to the results obtained in vitro, auto-ADP-ribosylated PARP-1 was detected in vivo with a maximum around ZT4 (Figures S1D–S1F).

Next, we asked whether rhythmic auto-ADP-ribosylation of PARP-1 is under the control of the circadian clock. Using nuclear extracts from mice with a conditionally active liver clock expressing REV-ERBα in the liver under the control of tetracycline-responsive elements (Tet-off system) (Kornmann et al., 2007), circadian auto-ADP-ribosylation levels of PARP-1 were found to be similar in the presence or absence of a functional clock

and dark phases, respectively. Each time point consists of a mixture of liver nuclear extracts obtained from three or four single animals. The bar diagrams show quantifications of the autoradiographies. See also Figure S1.

Figure 2. Circadian Auto-ADP-Ribosylation of PARP-1 in Mouse Liver Nuclear Extracts

(A) Analysis of auto-ADP-ribosylation of PARP-1 in wild-type mice fed ad libitum in the absence or presence of 40 μM of the PARG inhibitor ADP-HPD (Calbiochem).

(B) Assay for PARG activity in liver nuclear extracts. Recombinant human PARP-1 was pre-ADP-ribosylated in the presence of radiolabeled NAD^+ and then incubated with liver nuclear extracts obtained from wild-type mice supplemented with the PARP inhibitor PJ34. Auto-ADP-ribosylation was determined by autoradiography.

(C) Recombinant wild-type human PARP-1 was incubated alone or added to liver nuclear protein extracts obtained from *Parp-1* knockout mice sacrificed at 4 hr intervals around the clock, and its auto-ADP-ribosylation was determined by autoradiography.

(D) Quantification of recombinant PARP-1 auto-ADP-ribosylation incubated with three different sets of liver nuclear extracts obtained from *Parp-1* knockout mice fed ad libitum. Each set contains a mixture of extracts harvested from 2 or 3 mice per time point. Data represent the mean ± standard deviation (SD).

(E) Schematic representation of the different protein domains of PARP-1. The DNA-binding domain (DBD, amino acids 1–373) contains three zinc-binding motifs and is required for both the DNA binding and activation of the catalytic domain (CAT). The WGR domain (amino acids 525–656) is essential for enzyme activation. The catalytic domain (CAT, amino acids 656–1014) harbors the enzymatic activity and contains the NAD^+ binding site. It exhibits low basal activity when expressed alone. An additional loop domain (amino acids 476–525) harbors target amino acids for automodification and is required for full enzymatic activity. The BRCT domain (amino acids 385–476) is dispensable for enzymatic activity but is involved in protein-protein interactions (Altmeyer et al., 2009).

Nuclear extracts obtained from *Parp-1* knockout mice sacrificed at 4 hr intervals around the clock were reconstituted with (F) truncated recombinant PARP-1 (amino acids 533–1014) harboring the WGR and the catalytic domain or (G) recombinant PARP-1 lacking the BRCT domain (PARP-1 ΔBRCT), (lacking amino acids 385–476) and PARP-1 auto-ADP-ribosylation was determined by autoradiography. The bar diagrams show quantifications of the autoradiographies. See also Figure S2 and Figure S3.

(Figures 1C and 1D). As expected, REV-ERBα protein levels were oscillating in doxycycline-treated mice (Figure 1C) similar to wild-type mice (Figure 1A) and were constant in the absence of doxycycline in the clock-arrested mice (Figure 1D).

Maximal auto-ADP-ribosylation of PARP-1 occurred during the light phase, when mice usually rest and ingest little food. To examine whether auto-ADP-ribosylation of PARP-1 is regulated by feeding, liver extracts from mice fed exclusively during the circadian dark phase (night fed) or light phase (day fed) were prepared and analyzed. As expected, the peak of REV-ERBα expression was shifted by 12 hr in the day-fed animals compared to the night-fed control animals (Figures 1E and 1F). Maximal auto-ADP-ribosylation of PARP-1 was observed in night-fed animals during the circadian light phase (Figure 1E)

similarly to mice fed ad libitum (Figures 1A, 1C, and 1D and Figures S1A and S1D–S1F). In contrast, the peak of auto-ADP-ribosylation of PARP-1 was shifted by almost 12 hr in day-fed animals (Figure 1F and Figures S1G–S1I), suggesting that feeding regulates auto-ADP-ribosylation of PARP-1.

The rhythmic auto-ADP-ribosylation of PARP-1 could have been caused by circadian PARP-1 activity, circadian but antiphasic poly(ADP-ribose) glycohydrolase (PARG) activity, or a combination of both (Davidovic et al., 2001). Analysis of auto-ADP-ribosylation of PARP-1 in the presence of an inhibitor of PARG resulted in a general increase in PARP-1 auto-ADP-ribosylation levels; however the rhythmic pattern of activity was retained (Figure 2A). Furthermore, incubation of pre-auto-ADP-ribosylated recombinant PARP-1 with liver nuclear extracts

in the presence of a PARP inhibitor resulted in constant yet significantly lower auto-ADP-ribosylation levels of PARP-1 when compared to pre-auto-ADP-ribosylated PARP-1 incubated alone (Figure 2B). Therefore, we concluded that the daily changes in the auto-ADP-ribosylation levels of PARP-1 are most likely the result of circadian PARP-1, rather than PARG activity.

Circadian PARP-1 activity appeared to be clock independent and regulated by feeding. Remarkably, rhythmic auto-ADP-ribosylation of PARP-1 could be restored in vitro by the addition of equal amounts of recombinant PARP-1 to nuclear extracts obtained from *Parp-1* knockout animals (Figures 2C and 2D). This experiment suggested that liver nuclei contain a signal that can activate PARP-1 in a daytime-specific manner. NAD^+ levels seemed to be an attractive candidate for such a signal, as PARP-1 requires NAD^+ for its enzymatic activity and NAD^+ levels have been shown previously to be circadian (Nakahata et al., 2009; Ramsey et al., 2009). However, the circadian pattern of automodification of PARP-1 in nuclear liver extracts obtained from wild-type mice fed ad libitum persisted in the presence of 250 μM of unlabeled NAD^+ (Figures S2A and S2B). Furthermore, performing the experiment in the presence of 1 mM excess of NAD^+, this time using a poly(ADP-ribose) antibody to detect the levels of poly(ADP-ribosyl)ation, showed a daily pattern of activity similar to the one observed before for mice fed ad libitum, exclusively during the night or exclusively during the day (Figures S2C and S2D). Finally, circadian changes in NAD^+ levels were reported to be under the control of the circadian clock (Nakahata et al., 2009; Ramsey et al., 2009), whereas PARP-1 activity was clock independent (Figures 1C and 1D). Our results therefore argue against a scenario in which fluctuations in nuclear NAD^+ levels are solely responsible for the rhythmic PARP-1 activity in liver nuclear extracts.

Similar to what has been described previously, the presence of DNA turned out to be absolutely required for PARP-1 activity in vitro (Satoh and Lindahl, 1992). Both DNase treatment and the addition of the recombinant DNA-binding domain (DBD) of PARP-1 completely abolished PARP-1 auto-ADP-ribosylation (Figures S2E and S2F). Yet, neither DNA nor RNA seemed to determine the rhythmic properties of PARP-1 activity, as circadian PARP-1 activity persisted in the presence of an excess of exogenously added DNA (Figures S2G and S2H) or upon addition of equal amounts of DNA fragments following DNase treatment (Figure S2I) or following treatment with RNaseI (Figure S2J). Finally, zinc availability, which is required for the binding of the PARP-1 zinc fingers to DNA (Mazen et al., 1989), did not seem to participate in the regulation of daily PARP-1 activity (Figure S2K).

We further addressed known activation mechanisms that could lead to daily PARP-1 activity. Posttranslational modifications of PARP-1, such as acetylation (Hassa et al., 2005) or phosphorylation (Kauppinen et al., 2006), have been described to be involved in PARP-1 activation. However, neither pretreatment with the HDAC inhibitors Trichostatin A and Sirtinol (Figures S3A and S3B) nor in vitro preacetylation affected the circadian activity of PARP-1 (Figures S3C and S3D). Similarly, phosphatase pretreatment did not alter the pattern of PARP-1 auto-ADP-ribosylation in liver nuclear extracts (Figure S3E).

In an attempt to identify protein domains in PARP-1 that might be required for its circadian activity we utilized different deletion mutants of PARP-1 and analyzed their activity in liver nuclear extracts obtained from *Parp-1* knockout mice. In contrast to full-length recombinant PARP-1 (Figure 2C and Figure S3B), a truncated PARP-1 (amino acids 533–1014) or the PARP-1 ΔBRCT mutant that lacks amino acids 385–476 showed constant levels of activity around the day (Figures 2E–2G), suggesting that the BRCT domain, previously reported to be involved in protein-protein interactions (Mohammad and Yaffe, 2009), might be required for the circadian activity of PARP-1.

PARP-1 Binds to CLOCK-BMAL1 in a Daytime-Dependent Manner

Food intake serves as a strong *Zeitgeber* for peripheral clocks. Because cyclic PARP-1 activity was found to be regulated by feeding, we wanted to examine whether PARP-1 interacts directly with components of the molecular clock machinery. Immunoprecipitation of BMAL1 from mouse liver nuclear extracts resulted in coimmunoprecipitation of PARP-1 in a highly rhythmic fashion (Figures 3A and 3B). As a control, the interaction of BMAL1 with other core clock proteins was followed. As has been reported previously, the binding of BMAL1 to its dimerization partner CLOCK was almost constant throughout the day, whereas both PER2 and CRY1 exhibited circadian changes in their interaction with BMAL1 (Figure 3B) (Asher et al., 2008). In a reciprocal experiment, PARP-1 was immunoprecipitated from mouse liver nuclear extracts harvested around the clock. Here as well, BMAL1 coimmunoprecipitated with PARP-1 in a daily manner. The strength of the interaction was again maximal at the beginning of the light phase between ZT0 and ZT4; CLOCK was also detected at the same time points in a long exposure (Figure 3C). Finally, immunoprecipitation of CLOCK from mouse liver nuclear extracts from wild-type mice sacrificed at ZT4 and ZT16 resulted in coimmunoprecipitation of PARP-1 and BMAL1 specifically at ZT4 (Figure 3D).

To confirm the identity of PARP-1 in the immunoprecipitation experiments and to further characterize the interaction between CLOCK-BMAL1 and PARP-1, a similar experiment was conducted, this time with mouse liver nuclear extracts obtained from wild-type and *Parp-1* knockout mice sacrificed at ZT0. In both wild-type and PARP-1-deficient mice, immunoprecipitation of BMAL1 resulted in coimmunoprecipitation of CLOCK, indicating that the interaction between BMAL1 and CLOCK is not dependent on PARP-1 (Figure 3E). The absence of a PARP-1 signal in the *Parp-1* knockout mice confirmed the specificity of the PARP-1 antibody and the specific interaction of PARP-1 with CLOCK-BMAL1. Finally, the direct interaction of PARP-1 with CLOCK could also be reconstituted in vitro in a pull-down assay with purified recombinant proteins (Figure 3F).

PARP-1 Poly(ADP-Ribosyl)ates CLOCK in a Circadian Manner

PARP-1 has been described to modulate the activity of various transcriptional regulators either through protein-protein interactions or through poly(ADP-ribosyl)ation (Hassa et al., 2006; Kraus, 2008). We thus wished to determine whether the rhythmic interaction of PARP-1 with CLOCK-BMAL1 also leads to
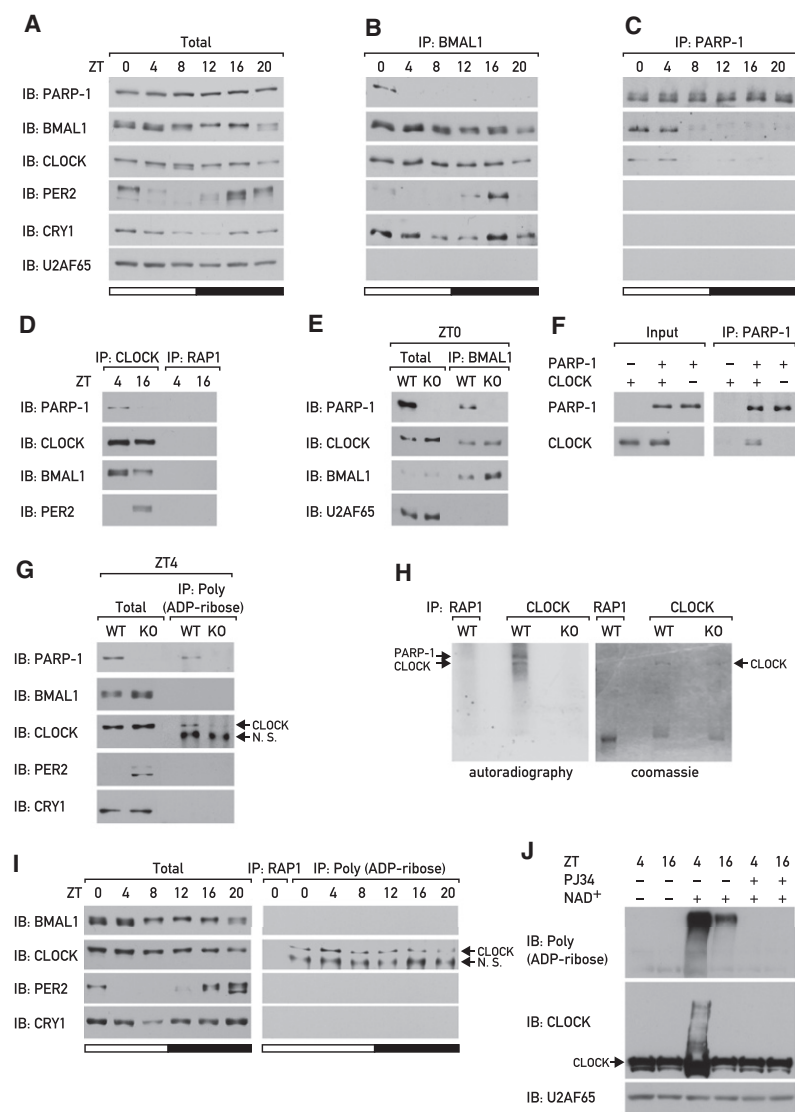
Figure 3. PARP-1 Binds and Poly(ADP-Ribosyl)ates CLOCK in a Circadian Manner

Mice were sacrificed at 4 hr intervals, and liver nuclear protein extracts were prepared.

(A) Protein extracts were analyzed by immunoblotting.

(B) BMAL1 and (C) PARP-1 were immunoprecipitated and the precipitated proteins were analyzed by immunoblotting.

(D) CLOCK was immunoprecipitated from liver nuclear extracts obtained from wild-type mice sacrificed at ZT4 and ZT16. An antibody against yeast RAP1 was used as a negative control.

(E) BMAL1 was immunoprecipitated from liver nuclear extracts obtained from wild-type and *Parp-1* knockout mice sacrificed at ZT0.

(F) Pull-down assay with recombinant CLOCK and HA-HIS-PARP-1. HA-HIS-PARP-1 was immunoprecipitated using mouse HA antibody.

(G) Wild-type and *Parp-1* knockout mice were sacrificed at ZT4, and mouse liver nuclear extracts were prepared and subjected to immunoprecipitation with rabbit poly(ADP-ribose) antibody (alx210-890, Alexis Biochemicals). The nonspecific (N.S.) band probably reflects an interaction of the secondary antibody with the heavy chain of the poly(ADP-ribose) antibody.

(H) CLOCK was immunoprecipitated from liver nuclear extracts from wild-type and *Parp-1* knockout mice and incubated with radioactively labeled NAD^+. An antibody against yeast RAP1 was used as a negative control. Immunoprecipitated proteins were analyzed by autoradiography and by Coomassie staining.

(I) Mouse liver nuclear extracts obtained from wild-type mice sacrificed at 4 hr intervals were subjected to immunoprecipitation with rabbit poly(ADP-ribose) antibody (alx210-890, Alexis Biochemicals), and with yeast RAP1 antibody as a negative control.

(J) Wild-type mice were sacrificed at ZT4 and ZT16, and mouse liver nuclear extracts were prepared and incubated either with NAD^+ alone or together with the PARP inhibitor PJ34 for 30 min at 30°C. Samples were separated by SDS gel electrophoresis and analyzed by immunoblotting. The asterisk marks the border between the stacking and the separating gel in the denaturing SDS gel.
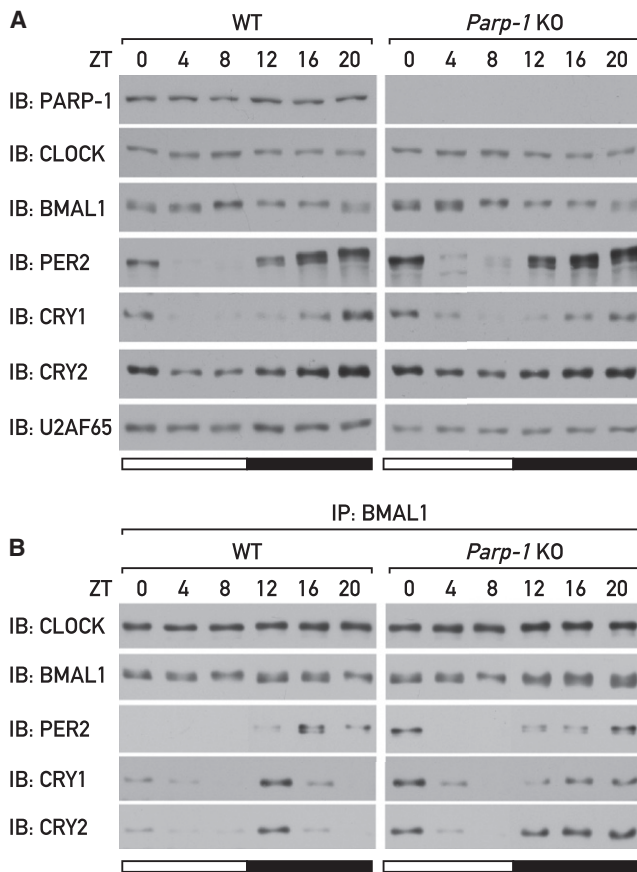
See also Figure S4.

PARP-1-dependent poly(ADP-ribosyl)ation of BMAL1 or CLOCK. Immunoprecipitation experiments were performed using a poly(ADP-ribose) antibody and liver nuclear extracts from wild-type and *Parp-1* knockout mice sacrificed at ZT4, the time point at which maximal interaction between CLOCK-BMAL1 and PARP-1 has been observed (Figures 1A–1D). CLOCK was immunoprecipitated much more efficiently from extracts harvested from wild-type as compared to *Parp-1* knockout mice, whereas the absolute levels of CLOCK were similar in both extracts (Figure 3G). Although auto-poly(ADP-ribosyl)ation of PARP-1 was also detected, no similar modification of BMAL1, PER2, or CRY1 could be identified (Figure 3G). To exclude the possibility that CLOCK precipitated due to binding to automodified PARP-1, extracts were treated with harsh denaturing conditions prior to the immunoprecipitation with the poly(ADP-ribose) antibody. Under these conditions similar results were obtained (Figure S4A).

In order to examine whether PARP-1 can directly poly(ADP-ribosyl)ate CLOCK, a cell-free system was employed. Equal amounts of CLOCK were immunoprecipitated from nuclear extracts of wild-type and PARP-1-deficient mice and incubated with radiolabeled NAD^+. The autoradiography revealed that CLOCK was ADP-ribosylated in a PARP-1-dependent manner (Figure 3H). Auto-ADP-ribosylation of PARP-1, which coimmunoprecipitated with CLOCK, was only observed in PARP-1 containing wild-type extracts. Taken together, our results suggested that PARP-1 can poly(ADP-ribosyl)ate CLOCK both in vitro and in vivo.

Finally, we wished to examine the temporal changes in poly(ADP-ribosyl)ation of CLOCK in vivo around the day. Remarkably, poly(ADP-ribosyl)ation of CLOCK was maximal at around ZT4 (Figure 3I and Figure S4B) and therefore coincided with the maximum of circadian binding of PARP-1 to CLOCK-BMAL1 (Figure 3) and maximal auto-ADP-ribosylation of PARP-1 (Figure 1 and Figure S1). Again, no similar modifications of CRY1, PER2, or BMAL1 were detected. These temporal changes in poly(ADP-ribosyl)ation of CLOCK were also observed

A

WT   *Parp-1* KO

ZT   0   4   8   12   16   20   0   4   8   12   16   20

IB: PARP-1

IB: CLOCK

IB: BMAL1

IB: PER2

IB: CRY1

IB: CRY2

IB: U2AF65

IP: BMAL1

B

WT   *Parp-1* KO

ZT   0   4   8   12   16   20   0   4   8   12   16   20

IB: CLOCK

IB: BMAL1

IB: PER2

IB: CRY1

IB: CRY2

Figure 4. Temporal Analysis of Core Clock Protein Expression Levels and Their Interactions in Wild-Type and *Parp-1* Knockout Mice

Wild-type and *Parp-1* knockout mice were sacrificed at 4 hr intervals around the clock, and liver nuclear protein extracts were prepared.

(A) Liver nuclear protein extracts were analyzed by immunoblotting.

(B) BMAL1 was immunoprecipitated from liver nuclear protein extracts and the immunoprecipitated proteins were analyzed by immunoblotting.

when liver nuclear extracts obtained from mice sacrificed at ZT4 and ZT16 were incubated with NAD$^+$, separated by SDS gel electrophoresis, and analyzed with a CLOCK antibody (Figure 3J). The accumulation of slower-migrating forms of CLOCK, specifically at ZT4 in the presence of NAD$^+$, was abolished upon addition of a PARP inhibitor (Figure 3J).

PARP-1 Modulates the Interaction of CLOCK-BMAL1 with Proteins of the Negative Limb

The circadian interaction of CLOCK-BMAL1 with PARP-1 and the rhythmic modification of CLOCK by PARP-1 encouraged us to examine the expression levels of nuclear core clock proteins and their interactions with each other in wild-type and *Parp-1* knockout mice around the clock. No significant differences in CLOCK, BMAL1, CRY1, and CRY2 protein levels between wild-type and *Parp-1* knockout extracts were observed (Figure 4A, see also Figures 3E and 3G). However, PER2 protein levels were slightly elevated in the absence of PARP-1, in partic-

ular during the light phase (ZT0–ZT8), (Figure 4A, see also Figure 3G).

Interestingly, when we performed immunoprecipitation experiments addressing the interaction of BMAL1 with other core clock proteins in wild-type and *Parp-1* knockout mice, temporal differences in the binding partners of BMAL1 became apparent (Figure 4B). Although no significant changes in the binding of BMAL1 to CLOCK could be observed, there were clear changes in the temporal interactions of PER2, CRY1, and CRY2 with CLOCK-BMAL1 (Figure 4B). At the beginning of the light phase (ZT0), the binding of PER2, CRY1, and CRY2 was elevated in the absence of PARP-1. Maximal binding of the negative limb members PER and CRY occurred at around ZT16 in wild-type mice, whereas in *Parp-1* knockout mice maximal binding was reached between ZT20 and ZT0 (Figure 4B). We concluded that PARP-1 modulated the interaction of CLOCK-BMAL1 with repressor components of the negative limb, possibly via poly(ADP-ribosyl)ation of CLOCK.

PARP-1 Reduces the DNA-Binding Activity of CLOCK-BMAL1

CLOCK-BMAL1 heterodimers exhibit rhythmic DNA binding to specific elements such as E boxes and G boxes (an E box variant) in the promoters of circadian target genes (Ripperger and Schibler, 2006; Yoo et al., 2005). As PARP-1-dependent poly(ADP-ribosyl)ation was reported previously to modulate the DNA-binding activity of several transcription factors (Kraus, 2008), we used electrophoretic mobility shift assays (EMSA) to examine the binding of CLOCK-BMAL1 to DNA in wild-type and *Parp-1* knockout mice. CLOCK-BMAL1 from wild-type liver extracts exhibited circadian binding to a radioactively labeled G box probe from the *Per2* promoter with maximal affinity around ZT8; in contrast, binding of CLOCK-BMAL1 appeared to be significantly stronger in PARP-1-deficient mice, particularly at ZT4 (Figure 5A and Figure S5B).

The EMSA experiment with the *Parp-1* knockout extracts further revealed a protein complex that runs faster than the CLOCK-BMAL1 complex and binds in a circadian fashion, however with a maximal binding around ZT12 (Figure 5A and Figure S5B). To get further insight into the composition and specificity of the different complexes we performed supershift assays and employed truncated/mutated G box probes or competitors (Figure S5 and Figure S6). As expected, the slower-migrating complex, which was previously reported to consist of CLOCK-BMAL1 (Reinke et al., 2008), was completely supershifted upon addition of specific antibodies against either BMAL1 or CLOCK (Figure S5C) and was abolished either using a mutated/deleted G box probe or in the presence of a G box competitor (Figure S5 and Figure S6). In contrast, the faster-migrating complex was not supershifted by CLOCK or BMAL1 antibodies and was not G box specific (Figures S5C–S5E). By using truncated variants of the G box probe in direct labeling as well as competition experiments, the binding site of this complex could be narrowed down to a short fragment containing a consensus SP1-binding site (Figure S5 and Figure S6). Moreover, point mutations in this site abolished the binding of the faster-migrating complex (Figures S5F–S5H), and the complex could be partially supershifted with an SP1 antibody
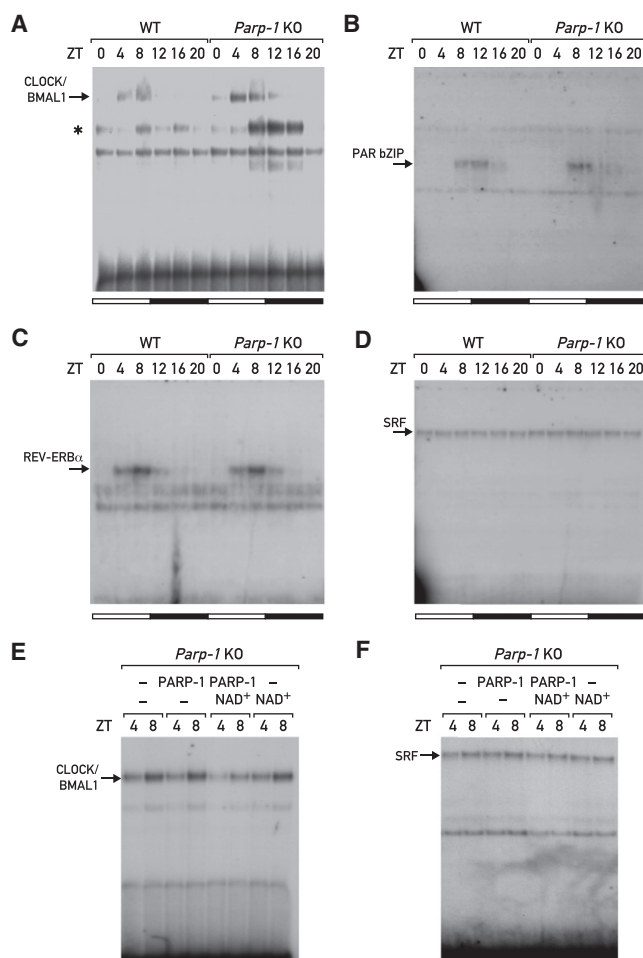
Figure 5. Analysis of the DNA Binding of CLOCK-BMAL1 Complexes in Nuclear Extracts from Wild-Type and *Parp-1* Knockout Mice

Liver nuclear protein extracts obtained from wild-type and *Parp-1* knockout mice sacrificed at 4 hr intervals around the clock were analyzed by EMSA using different probes.

(A) G box probe. (B) PAR bZIP probe. (C) REV-ERBα probe and (D) SRF probe. Liver nuclear protein extracts obtained from *Parp-1* knockout mice sacrificed at ZT4 and ZT8 were incubated without or with recombinant PARP-1, NAD$^+$, or both reagents together and subsequently analyzed by EMSA using (E) a G box probe and (F) an SRF probe. The asterisk marks a protein-DNA complex that is seen preferentially with liver nuclear extracts from *Parp-1* knockout mice. As analyzed in Figure S5 and Figure S6, this complex contains the transcription factor SP1.

See also Figure S5.

(Figure S6E). These findings are in line with previous reports claiming that ADP-ribosylation of SP1 by PARP-1 impairs its DNA-binding activity (Zaniolo et al., 2007) and that SP1 can bind DNA in a daily manner (Reinke et al., 2008).

Next, we examined the DNA binding of other known transcription factors by using EMSA probes specific for circadian (PAR bZIP and REV-ERBα) and constitutively expressed (SRF) transcription factors. The binding of these proteins to their cognate DNA sequences was not significantly affected in the absence of PARP-1 (Figures 5B–5D).

We employed a cell-free assay to further investigate the possible role of PARP-1 in the DNA-binding activity of CLOCK-BMAL1. Liver nuclear extracts from *Parp-1* knockout mice were incubated with PARP-1 and NAD$^+$ alone or with both reagents together, and the DNA binding of CLOCK-BMAL1 was subsequently analyzed by EMSA. Only upon addition of both recombinant PARP-1 and NAD$^+$ did we observe a significant decrease in the binding of CLOCK-BMAL1 to DNA (Figure 5E). The same experiment performed with a DNA probe for SRF exhibited only a slight impairment in the DNA-binding activity of SRF (Figure 5F). Taken together our findings suggested that poly(ADP-ribosyl)ation of CLOCK, or the association of CLOCK with ADP-ribosylated PARP-1, attenuates the binding of CLOCK-BMAL1 to DNA.

Food Entrainment of Peripheral Circadian Clocks Is Impaired in PARP-1-Deficient Mice

The feeding-dependent changes in daily PARP-1 activity and the PARP-1-dependent poly(ADP-ribosyl)ation of CLOCK incited us to investigate whether PARP-1 might participate in the food entrainment of peripheral clocks. If this was indeed the case, the kinetics of feeding-dependent phase inversion would be expected to be altered in *Parp-1* knockout mice (for explanations, see Kornmann et al., 2007). To test this hypothesis, wild-type and PARP-1-deficient animals were first fed ad libitum (which corresponds largely to night feeding), and mice were sacrificed every 4 hr. After a few weeks of ad libitum feeding, the feeding regimen was changed, and food was offered to the animals exclusively during the day. Starting 24 hr after changing the feeding regimen, animals were sacrificed every 4 hr during 80 hr. Transcript levels of core clock genes under feeding ad libitum and during the adaptation period to the day-feeding regimen were determined by analyzing mRNA levels using real-time quantitative PCR.

In animals fed ad libitum, no dramatic changes in gene expression between wild-type and PARP-1-deficient mice were observed. Nevertheless at ZT4, the time when we observed maximal PARP-1 activity and CLOCK ADP-ribosylation, we did notice in *Parp-1* knockout mice somewhat decreased mRNA expression levels of genes (*Dbp*, *Dec1*, and *Dec2*) that have been reported to be direct target genes of CLOCK-BMAL1 (Figure 6 and Figure S7).

Interestingly, upon changing to day feeding, we could observe different adaption kinetics for different genes even in the wild-type background. In particular, the expression of *Per2* adapted more quickly to daytime feeding than other tested genes (Figure 6). Remarkably, however, there was a clear difference in the expression of all genes examined (*Per1*, *Per2*, *Cry1*, *Rorγ*, *Bmal1*, *Rev-Erbα*, and *Dbp*) between *Parp-1* knockout animals and their wild-type littermates (Figure 6). For example, *Per1*, *Per2*, *Cry1*, and *Rorγ* showed a phase delay in expression levels in *Parp-1* knockout mice compared to wild-type mice of up to 8 hr after 4 days of food shifting. The adaptation phase of the other genes examined in *Parp-1* knockout mice was also slower. Taken together our analysis suggests that PARP-1 contributes to the adaptation of circadian gene expression to food entrainment in mouse liver.
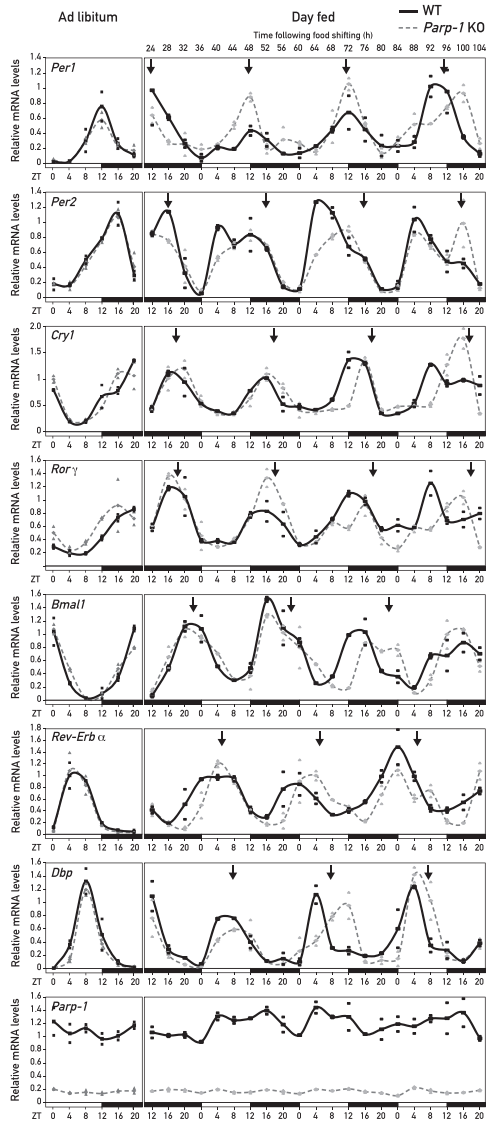
Figure 6. Temporal Analysis of mRNA Levels of Core Clock Genes in Wild-Type and *Parp-1* Knockout Mice in Animals Fed Ad Libitum or Fed Exclusively during the Day

Wild-type and *Parp-1* knockout mice were first fed ad libitum. After a few weeks, the feeding regimen was changed and food was offered exclusively during the light phase. Starting 24 hr after changing the feeding regimen, animals were sacrificed every 4 hr during 80 hr. Total RNA was prepared from liver and mRNA expression levels of *Per1*, *Per2*, *Cry1*, *Rorγ*, *Bmal1*, *Rev-Erbα*, *Dbp*, and *Parp-1* were determined by quantitative TaqMan real-time PCR. Data points connected by a line present the mean values obtained from two or three single mice per time point. Single mice values are shown as black squares for wild-type mice and gray triangles for knockout mice. Arrows indicate the time points of maximal expression of the respective genes in mice fed ad libitum. See also Figure S7.

Parp-1 Knockout Mice Exhibit Altered Circadian Rhythms of Locomotor Activity in Response to Restricted Feeding

Our findings suggested a role for PARP-1 in connecting feeding to circadian rhythmicity in the liver. We wished to examine

whether PARP-1 also affects the master clock in the brain and recorded the locomotor activity of wild-type and *Parp-1* knockout mice under different light and feeding regimens. Under 12 hr light–12 hr dark conditions, we did not observe any differences between *Parp-1* knockout mice and their wild-type littermates, neither in the activity pattern nor in overall locomotor activity (Figures 7A–7B and 7H). In contrast, under free-running conditions in constant darkness, *Parp-1* knockout mice exhibited a small but statistically significant lengthening of their circadian period (wild-type mice 23.51 ± 0.144; *Parp-1* knockout mice 23.78 ± 0.138; p value 0.002) (Figures 7A–7D). This suggested that PARP-1 also modulates to some extent the function of the master clock in the brain. We did not observe any differences in wheel-running behavior under constant light conditions (data not shown). Analysis of the food anticipatory activity (FAA) of wild-type and *Parp-1* knockout mice upon exposure to restricted feeding during the light phase (ZT3–ZT9) did not reveal any significant differences in FAA (Figures 7E–7H). We noted, however, that upon restricted feeding, *Parp-1* knockout mice were markedly more active during most of the dark phase compared to their wild-type littermates, whereas no significant differences were observed when food was provided ad libitum (Figures 7E–H).

DISCUSSION

PARP-1-Dependent Poly(ADP-Ribosyl)ation Modulates the Activity of CLOCK

Over the past years, a variety of modifications such as phosphorylation, acetylation, sumoylation, and others have been shown to modulate circadian gene expression (Gallego and Virshup, 2007). We have shown here that CLOCK appears to be a target of yet another posttranslational modification, namely poly(ADP-ribosyl)ation by PARP-1, and that this modification might affect CLOCK function at multiple levels.

PARP-1 seems to be a feeding-dependent regulator of the circadian clock. In mice fed ad libitum, feeding occurs mainly during the dark phase, and as a result, PARP-1 activity is low during the dark and increases during the light phase. At around ZT4, we observed maximal auto-ADP-ribosylation of PARP-1, maximal binding of PARP-1 to CLOCK-BMAL1, and maximal poly(ADP-ribosyl)ation of CLOCK. The daytime-specific interaction of CLOCK-BMAL1 with PARP-1 and the poly(ADP-ribosyl)ation of CLOCK were accompanied by temporal changes in the binding of CLOCK-BMAL1 to PER and CRY repressor proteins and an impaired affinity of the CLOCK-BMAL1 heterodimer for its DNA recognition sequences. Although the DNA-binding activity of CLOCK-BMAL1 was enhanced in PARP-1-deficient mice at ZT4, the increased recruitment of repressor proteins of the negative limb, such as PER and CRY, probably led to a net decrease in the transcription of direct CLOCK-BMAL1 target genes.

PARP-1 Participates in the Phase Entrainment of Peripheral Oscillators to Feeding

Daily feeding-fasting cycles are dominant *Zeitgebers* for peripheral clocks (Damiola et al., 2000; Stokkan et al., 2001), but the involved molecular signaling pathways are poorly understood
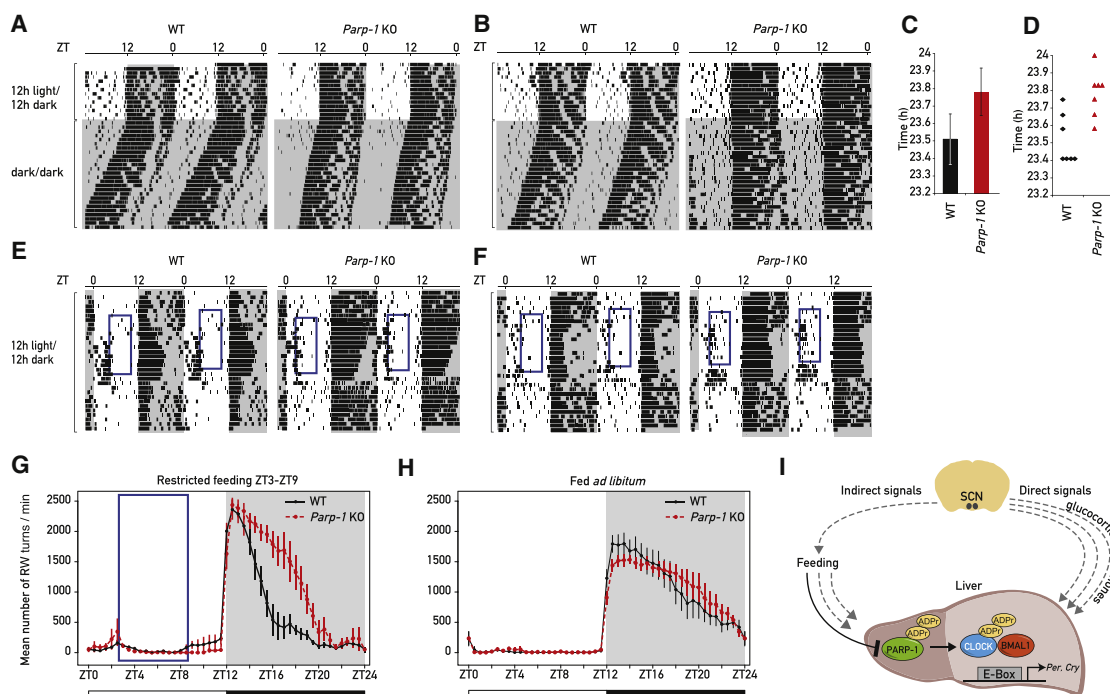
Figure 7. Analysis of the Circadian Locomotor Activity and Food Anticipatory Activity (FAA) of Wild-Type and *Parp-1* Knockout Mice

(A and B) The locomotor activity of mice lacking PARP-1 (*Parp-1* KO) and their wild-type littermates (WT) was recorded as wheel-running activity. Representative double-plot actograms obtained for two animals of each genotype are shown. In each actogram the first few days were recorded under 12 hr light-12 hr dark conditions, after which the light was turned off and recording was continued in constant darkness. Time spans during which the lights were switched off are marked by gray shading.

(C) Period lengths of wild-type and *Parp-1* knockout mice in constant darkness. Free-running period lengths in hours were 23.51 ± 0.144 (wild-type) and 23.78 ± 0.138 (*Parp-1* knockout). The bar diagram represents the mean $\pm$ SD. The Student's t test was used to examine the data; the p value for the period length difference was 0.002.

(D) Period length distribution in constant darkness for wild-type and *Parp-1* knockout mice.

(E and F) FAA of mice lacking PARP-1 (*Parp-1* KO) and their wild-type littermates (WT) was recorded as wheel-running activity. Representative double-plot actograms obtained for two animals of each genotype are shown. Activity was recorded under 12 hr light-12 hr dark conditions. During the first few days, food was provided ad libitum, then animals received for 12 days 80% of their normal food consumption between ZT3 and ZT9; subsequently food was again provided ad libitum.

(G) Percentage of mean activity during a 24 hr period for animals subjected to temporally restricted feeding (ZT3–ZT9). Mean values $\pm$ standard error of the mean (SEM) obtained from five animals of each genotype (recorded between day 3 and day 12 after the onset of restricted feeding) are shown.

(H) Percentage of mean activity during a 24 hr period for animals subjected to feeding ad libitum. Mean values $\pm$ SEM obtained from seven animals of each genotype recorded for 9 consecutive days. Time spans during which restricted feeding occurred are outlined in blue.

(I) The SCN synchronizes cellular circadian oscillators in liver (and other peripheral tissues) indirectly through circadian behavior (i.e., feeding-fasting rhythms) and more directly (e.g., via controlling cyclic hormone secretion). PARP-1 activity, which is regulated by daily feeding cycles, affects the molecular clockwork by poly (ADP-ribosyl)ating CLOCK. As feeding inversion does not affect the phase of the SCN, the direct *Zeitgeber* signals emanating from the SCN (direct signals) are in conflict with the ones associated with feeding (indirect signals) upon inverting the phase of feeding. The phase inversion kinetics in liver depends on the competition between direct and indirect *Zeitgeber* signals. If one (or more) of the direct signaling pathways are inactivated, the food-regimen-induced phase inversion is accelerated (as in the case for mice with liver-specific glucocorticoid receptor null alleles, see Le Minh et al., 2001). Conversely, if a feeding-dependent pathway is impaired, the kinetics of food-regimen-induced phase inversion is slowed down, as in the case of PARP-1-deficient mice.

and probably redundant. Owing to this redundancy, the impact of a single signaling pathway can probably only be measured when phase-shifting kinetics during the transition from the old to the new phase are recorded. Proof-of-concept for this approach has been reported for the synchronization of liver circadian oscillators by glucocorticoid hormones (Le Minh et al., 2001; for review, see Kornmann et al., 2007). Such experiments now revealed that, at least in the liver, PARP-1 appears to be involved in a pathway connecting feeding to circadian oscillators. PARP-1 might convey signals associated with the feeding status to the circadian oscillator via poly(ADP-ribosyl)ation of

CLOCK, thus in the absence of PARP-1 the hepatocyte oscillators adapt slower to an altered feeding regimen (Figure 7I).

Interestingly, in wild-type animals core clock and clock-controlled genes can differ in their responding kinetics to food entrainment. For example, *Per2*, *Cry1*, and *Rorγ* adapt their expression faster to the new feeding regimen, and kinetics of food entrainment of these genes also showed the most pronounced differences between wild-type and *Parp-1* knockout animals. In contrast, *Per1, Rev-Erbα*, and *Dbp* adjusted their expression considerably slower to the new phase. Conceivably, in peripheral organs such as the liver, some clock

genes (e.g., *Per1*, *Rev-Erbα*, and *Dbp*) are strongly responsive to regulatory cues from the SCN, whereas others (e.g., *Per2*, *Cry1*, and *Rorγ*) are more susceptible to food-derived signals. *Per2* is a strong candidate for a core clock gene whose expression is responsive to feeding-dependent cues. First, the phase of its expression responds rapidly to food shifting, and second, in a mouse model with conditionally active liver clocks, *Per2* was identified as a system-driven gene, i.e., as a gene whose expression continues to be cyclic in the liver in the absence of functional hepatocyte oscillators (Kornmann et al., 2007).

Circadian PARP-1 Activity

What are the signals generated by feeding-fasting cycles and leading to the daily activation of PARP-1 and subsequently poly(ADP-ribosyl)ation of CLOCK? As PARP-1 activity is NAD$^+$ dependent, one could speculate that it correlates with cellular NAD$^+$ levels. Previous studies have indeed shown that the NAD$^+$ levels in mammals are cycling during the day (Nakahata et al., 2009; Ramsey et al., 2009). Circadian NAD$^+$/NADH levels might therefore determine the activity of PARP-1, leading to daily changes in the poly(ADP-ribosyl)ation of CLOCK. However, this is unlikely to be the sole cause for circadian PARP-1 activity in vivo, as an excess of NAD$^+$ does not affect circadian PARP-1 activity in vitro. Moreover, circadian changes in NAD$^+$ levels were reported to be under the control of circadian oscillators (Nakahata et al., 2009; Ramsey et al., 2009), whereas rhythmic PARP-1 activity persisted in hepatocytes without functional oscillators. As the circadian activation of PARP-1 could be reconstituted in the test tube with recombinant PARP-1 and temporally staged nuclear extracts, we consider it likely that the underlying mechanism involves macromolecules that remain associated with the nuclei during their purification. It will be an enticing, but challenging task to identify these molecules and the signaling cascade leading to the daily activity of PARP-1.

EXPERIMENTAL PROCEDURES

RNA Analysis by Real-Time Quantitative PCR

RNA extraction and transcript quantification by TaqMan real-time PCR technology were performed as previously described (Preitner et al., 2002). Real-time PCR data were normalized to *Eef1a1* and *mTbp* and relative mRNA levels were calculated using the GeNorm method (Vandesompele et al., 2002). Primers and probes are listed in Table S1.

Protein Extraction and Immunoblot Analysis

Proteins from mouse liver nuclei were prepared according to the NUN procedure (Lavery and Schibler, 1993). SDS gel and immunoblot analysis were performed according to standard protocols. Antibodies used were rabbit CRY1, CRY2, PER2, REV-ERBα, BMAL1, and CLOCK (kindly provided by S. Brown and J. Ripperger); rabbit PARP-1 (H-250, Santa Cruz); rabbit poly(ADP-ribose) (alx210-890, Alexis biochemicals or LP-96-10, BD); mouse poly(ADP-ribose) (alx804-220, mAb [10H], Alexis Biochemicals); rabbit PCNA (Santa Cruz); and mouse U2AF65 and mouse HA (Sigma).

PARP-1 Activity Assays in Mouse Liver Nuclear Extracts

Five micrograms of mouse liver nuclear extract was diluted in 25 μl reaction buffer (50 mM Tris-HCl, pH 8.0, 4 mM MgCl$_2$, 250 μM DTT, 1 μg/ml pepstatin, 1 μg/ml bestatin, 1 μg/ml leupeptin, 250 nM ^{32}P-NAD) and incubated for 30 min at 30°C. Proteins were separated by SDS-PAGE and ADP-ribosylation was analyzed by autoradiography. PARP-1 auto-ADP-ribosylation was quantified using the software ImageJ 1.42q.

Coimmunoprecipitation Experiments

Coimmunoprecipitation experiments were carried out with mouse liver nuclear extracts. Extracts were incubated for 12 hr with the indicated antibodies at 4°C and further incubated with protein A beads (Roche) for an additional 2 hr at 4°C. The beads were collected by centrifugation and washed with NP-40 buffer (100 mM Tris-HCL, pH 7.5, 150 mM NaCl, 2 mM EDTA, and 1% NP-40). Laemmli sample buffer was added and samples were heated at 95°C for 5 min and separated on a polyacrylamide-SDS gel.

EMSA

EMSA reactions were performed with 5 μg of nuclear proteins in 25 mM HEPES-KOH (pH 7.6), 150 mM NaCl, 0.1 mM EDTA, 1 mM DTT, 200 ng/μl sheared salmon sperm DNA, 50 ng/μl poly(dI-dC), and 1 μl of radioactive probe in a volume of 10 μl. One microliter of loading dye (15% Ficoll, 0.4% Orange G) was added, and the reaction mixes were loaded on 4% polyacrylamide gels. Gels were run for 3 hr at room temperature (7.5 V/cm), vacuum-dried, and exposed on a film. Supershift experiments were performed with 1 μl of purified antibody added into the reaction before adding the radioactive probe. The sequences of the EMSA probes are listed in Table S2.

REFERENCES

Altmeyer, M., and Hottiger, M.O. (2009). Poly(ADP-ribose) polymerase 1 at the crossroad of metabolic stress and inflammation in aging. Aging (Albany NY) *1*, 458–469.

Altmeyer, M., Messner, S., Hassa, P.O., Fey, M., and Hottiger, M.O. (2009). Molecular mechanism of poly(ADP-ribosyl)ation by PARP1 and identification of lysine residues as ADP-ribose acceptor sites. Nucleic Acids Res. *37*, 3723–3738.

Asher, G., Gatfield, D., Stratmann, M., Reinke, H., Dibner, C., Kreppel, F., Mostoslavsky, R., Alt, F.W., and Schibler, U. (2008). SIRT1 regulates circadian clock gene expression through PER2 deacetylation. Cell *134*, 317–328.

Damiola, F., Le Minh, N., Preitner, N., Kornmann, B., Fleury-Olela, F., and Schibler, U. (2000). Restricted feeding uncouples circadian oscillators in peripheral tissues from the central pacemaker in the suprachiasmatic nucleus. Genes Dev. *14*, 2950–2961.

Davidovic, L., Vodenicharov, M., Affar, E.B., and Poirier, G.G. (2001). Importance of poly(ADP-ribose) glycohydrolase in the control of poly(ADP-ribose) metabolism. Exp. Cell Res. *268*, 7–13.

Dodd, A.N., Gardner, M.J., Hotta, C.T., Hubbard, K.E., Dalchau, N., Love, J., Assie, J.M., Robertson, F.C., Jakobsen, M.K., Goncalves, J., et al. (2007). The Arabidopsis circadian clock incorporates a cADPR-based feedback loop. Science *318*, 1789–1792.

Gallego, M., and Virshup, D.M. (2007). Post-translational modifications regulate the ticking of the circadian clock. Nat. Rev. Mol. Cell Biol. *8*, 139–148.

Green, C.B., Takahashi, J.S., and Bass, J. (2008). The meter of metabolism. Cell *134*, 728–742.

Hardin, P.E., Hall, J.C., and Rosbash, M. (1990). Feedback of the Drosophila period gene product on circadian cycling of its messenger RNA levels. Nature *343*, 536–540.

Hassa, P.O., and Hottiger, M.O. (2008). The diverse biological roles of mammalian PARPS, a small but powerful family of poly-ADP-ribose polymerases. Front. Biosci. *13*, 3046–3082.

Hassa, P.O., Haenni, S.S., Buerki, C., Meier, N.I., Lane, W.S., Owen, H., Gersbach, M., Imhof, R., and Hottiger, M.O. (2005). Acetylation of poly(ADP-ribose) polymerase-1 by p300/CREB-binding protein regulates coactivation of NF-kappaB-dependent transcription. J. Biol. Chem. *280*, 40450–40464.

Hassa, P.O., Haenni, S.S., Elser, M., and Hottiger, M.O. (2006). Nuclear ADP-ribosylation reactions in mammalian cells: where are we today and where are we going? Microbiol. Mol. Biol. Rev. *70*, 789–829.

Kauppinen, T.M., Chan, W.Y., Suh, S.W., Wiggins, A.K., Huang, E.J., and Swanson, R.A. (2006). Direct phosphorylation and regulation of poly(ADP-ribose) polymerase-1 by extracellular signal-regulated kinases 1/2. Proc. Natl. Acad. Sci. USA *103*, 7136–7141.

Kornmann, B., Schaad, O., Bujard, H., Takahashi, J.S., and Schibler, U. (2007). System-driven and oscillator-dependent circadian transcription in mice with a conditionally active liver clock. PLoS Biol. *5*, e34.

Kraus, W.L. (2008). Transcriptional control by PARP-1: chromatin modulation, enhancer-binding, coregulation, and insulation. Curr. Opin. Cell Biol. *20*, 294–302.

Lavery, D.J., and Schibler, U. (1993). Circadian transcription of the cholesterol 7 alpha hydroxylase gene may involve the liver-enriched bZIP protein DBP. Genes Dev. *7*, 1871–1884.

Le Minh, N., Damiola, F., Tronche, F., Schutz, G., and Schibler, U. (2001). Glucocorticoid hormones inhibit food-induced phase-shifting of peripheral circadian oscillators. EMBO J. *20*, 7128–7136.

Mazen, A., Menissier-de Murcia, J., Molinete, M., Simonin, F., Gradwohl, G., Poirier, G., and de Murcia, G. (1989). Poly(ADP-ribose)polymerase: a novel finger protein. Nucleic Acids Res. *17*, 4689–4698.

Mohammad, D.H., and Yaffe, M.B. (2009). 14-3-3 proteins, FHA domains and BRCT domains in the DNA damage response. DNA Repair (Amst.) *8*, 1009–1017.

Nakahata, Y., Kaluzova, M., Grimaldi, B., Sahar, S., Hirayama, J., Chen, D., Guarente, L.P., and Sassone-Corsi, P. (2008). The NAD+-dependent deacetylase SIRT1 modulates CLOCK-mediated chromatin remodeling and circadian control. Cell *134*, 329–340.

Nakahata, Y., Sahar, S., Astarita, G., Kaluzova, M., and Sassone-Corsi, P. (2009). Circadian control of the NAD+ salvage pathway by CLOCK-SIRT1. Science *324*, 654–657.

Panda, S., Poirier, G.G., and Kay, S.A. (2002). tej defines a role for poly(ADP-ribosyl)ation in establishing period length of the *Arabidopsis* circadian oscillator. Dev. Cell *3*, 51–61.

Petesch, S.J., and Lis, J.T. (2008). Rapid, transcription-independent loss of nucleosomes over a large chromatin domain at Hsp70 loci. Cell *134*, 74–84.

Preitner, N., Damiola, F., Lopez-Molina, L., Zakany, J., Duboule, D., Albrecht, U., and Schibler, U. (2002). The orphan nuclear receptor REV-ERBalpha controls circadian transcription within the positive limb of the mammalian circadian oscillator. Cell *110*, 251–260.

Ramsey, K.M., Yoshino, J., Brace, C.S., Abrassart, D., Kobayashi, Y., Marcheva, B., Hong, H.K., Chong, J.L., Buhr, E.D., Lee, C., et al. (2009). Circadian clock feedback cycle through NAMPT-mediated NAD+ biosynthesis. Science *324*, 651–654.

Reinke, H., Saini, C., Fleury-Olela, F., Dibner, C., Benjamin, I.J., and Schibler, U. (2008). Differential display of DNA-binding proteins reveals heat-shock factor 1 as a circadian transcription factor. Genes Dev. *22*, 331–345.

Reppert, S.M., and Weaver, D.R. (2002). Coordination of circadian timing in mammals. Nature *418*, 935–941.

Ripperger, J.A., and Schibler, U. (2006). Rhythmic CLOCK-BMAL1 binding to multiple E-box motifs drives circadian Dbp transcription and chromatin transitions. Nat. Genet. *38*, 369–374.

Rutter, J., Reick, M., Wu, L.C., and McKnight, S.L. (2001). Regulation of clock and NPAS2 DNA binding by the redox state of NAD cofactors. Science *293*, 510–514.

Sato, T.K., Panda, S., Miraglia, L.J., Reyes, T.M., Rudic, R.D., McNamara, P., Naik, K.A., FitzGerald, G.A., Kay, S.A., and Hogenesch, J.B. (2004). A functional genomics strategy reveals Rora as a component of the mammalian circadian clock. Neuron *43*, 527–537.

Satoh, M.S., and Lindahl, T. (1992). Role of poly(ADP-ribose) formation in DNA repair. Nature *356*, 356–358.

Schreiber, V., Dantzer, F., Ame, J.C., and de Murcia, G. (2006). Poly(ADP-ribose): novel functions for an old molecule. Nat. Rev. Mol. Cell Biol. *7*, 517–528.

Stokkan, K.A., Yamazaki, S., Tei, H., Sakaki, Y., and Menaker, M. (2001). Entrainment of the circadian clock in the liver by feeding. Science *291*, 490–493.

Vandesompele, J., De Preter, K., Pattyn, F., Poppe, B., Van Roy, N., De Paepe, A., and Speleman, F. (2002). Accurate normalization of real-time quantitative RT-PCR data by geometric averaging of multiple internal control genes. Genome Biology *3*, RESEARCH0034.

Yagita, K., Tamanini, F., van Der Horst, G.T., and Okamura, H. (2001). Molecular mechanisms of the biological clock in cultured fibroblasts. Science *292*, 278–281.

Yoo, S.H., Ko, C.H., Lowrey, P.L., Buhr, E.D., Song, E.J., Chang, S., Yoo, O.J., Yamazaki, S., Lee, C., and Takahashi, J.S. (2005). A noncanonical E-box enhancer drives mouse Period2 circadian oscillations in vivo. Proc. Natl. Acad. Sci. USA *102*, 2608–2613.

Zaniolo, K., Desnoyers, S., Leclerc, S., and Guerin, S.L. (2007). Regulation of poly(ADP-ribose) polymerase-1 (PARP-1) gene expression through the post-translational modification of Sp1: a nuclear target protein of PARP-1. BMC Mol. Biol. *8*, 96.